HHS Public Access

Author manuscript

Biomaterials. Author manuscript; available in PMC 2017 March 01.

Published in final edited form as:

Biomaterials. 2016 March ; 83: 257–268. doi:10.1016/j.biomaterials.2016.01.021.

Localized Delivery of Low-Density Lipoprotein Docosahexaenoic Acid Nanoparticles to the Rat Brain using Focused Ultrasound

Rohit S. Mulik[1], **Chenchen Bing**[2], **Michelle Ladouceur-Wodzak**[2], **Imalka Munaweera**[2], **Rajiv Chopra**[1,2], and **Ian R. Corbin**[1,3,*]

[1]Advanced Imaging Research Center, University of Texas Southwestern Medical Center at Dallas, Dallas, TX 75390, USA

[2]Radiology, University of Texas Southwestern Medical Center at Dallas, Dallas, TX 75390, USA

[3]Internal Medicine, University of Texas Southwestern Medical Center at Dallas, Dallas, TX 75390, USA

Abstract

Focused ultrasound exposures in the presence of microbubbles can achieve transient, non-invasive, and localized blood-brain barrier (BBB) opening, offering a method for targeted delivery of therapeutic agents into the brain. Low-density lipoprotein (LDL) nanoparticles reconstituted with docosahexaenoic acid (DHA) could have significant therapeutic value in the brain, since DHA is known to be neuroprotective. BBB opening was achieved using pulsed ultrasound exposures in a localized brain region in normal rats, after which LDL nanoparticles containing the fluorescent probe DiR (1,1′-Dioctadecyl-3,3,3′,3′-Tetramethylindotricarbocyanine Iodide) or DHA were administered intravenously. Fluorescent imaging of brain tissue from rats administered LDL-DiR demonstrated strong localization of fluorescence signal in the exposed hemisphere. LDL-DHA administration produced 2× more DHA in the exposed region of the brain, with a corresponding increase in Resolvin D1 levels, indicating DHA was incorporated into cells and metabolized. Histological evaluation did not indicate any evidence of increased tissue damage in exposed brain regions compared to normal brain. This work demonstrates that localized delivery of DHA to the brain is possible using systemically-administered LDL nanoparticles combined with pulsed focused ultrasound exposures in the brain. This technology could be used in regions of acute brain injury or as a means to target infiltrating tumor cells in the brain.

Introduction

To date, drug delivery to the brain remains a challenging task. The blood-brain barrier (BBB) located at the level of cerebral capillaries protects the brain by restricting free movement of most small and large molecules between the systemic circulation and neuronal

*Correspondence should be addressed to: Dr. Ian R. Corbin, Advanced Imaging Research Center, 5323 Harry Hines Blvd., Dallas, Texas, 75390, Phone: 214-645-7044; Fax: 214-645-2744; ian.corbin@utsouthwestern.edu.

tissue. Only a small subset of molecules of correct size (<400 Da), charge and lipid solubility can traverse the BBB in appreciable amounts.[1] Anatomically the BBB is made up primarily of unique endothelial cells found within the capillary network of the CNS. The basal and inner membranes of these endothelial cells are closely associated with foot processes of adjacent astrocytes.[2] BBB endothelial cells differ from those in the periphery as they essentially have no fenestrae and show little bulk vesicular transport. Furthermore, adjacent cells are tightly adherent, so little to no paracellular molecular diffusion occurs.[3, 4]

A number of different approaches have been developed to overcome the BBB for delivery of diagnostic or therapeutic agents into the CNS. These approaches include: biopharmaceutical modification to drugs to enable them to cross the BBB via endogenous transport mechanisms[5]; chemical permeation with high concentration mannitol[6]; use of cell penetrating peptides[7]; or even direct access to the brain via infusion cannulae.[8] These strategies have also been combined with various drug delivery vehicles such as liposomes[9], colloidal carriers[10, 11] and supramolecular aggregates[12] to deliver greater quantities of bioactive or contrast agents to the brain. However, all of these methods suffer from being either non-targeted or invasive. The application of focused ultrasound (FUS) coupled with IV administration of microbubbles is a unique method whereby localized opening of the BBB can be achieved in a non-invasive manner.[13] Low-intensity pulsed FUS exposures delivered to brain regions with circulating intravascular microbubbles cause the microbubbles within the path of the acoustic beam to interact with the endothelial lining. The mechanism governing the interactions between the microbubbles and their surrounding endothelial cells is thought to arise from radiation force and/or shear stress on the blood vessel walls when the microbubbles oscillate in response to the acoustic stimulus, leading to opening of the BBB through physiological and cellular processes.[14-16] This opening of the BBB is transient (half-life of BBB opening is 2-3 hrs),[17] reversible and nondestructive.[18] Furthermore, gap sizes up to 65 um can be achieved after FUS exposures [15] and molecules up to 2 MDa in size have been shown to cross the BBB [19], thus enabling macromolecules and nanoparticles to gain access to the CNS.

In recent decades, there has been great interest in utilizing nanoparticles as delivery vehicles for drug and imaging agents.[20] These nanostructures are typically synthetic platforms constructed from inorganic or polymeric materials.[21] Nanoparticle selection for drug delivery to the brain is a critical decision, as neurotoxicity remains a limiting factor not only for the drug cargo but also for nanoparticle vehicle.[22] Lipoproteins are endogenous lipid transporters within the circulation that shuttle cholesterol and triglycerides between various tissues in the body. Our group and others have shown that these lipid carriers can be isolated from plasma, modified with imaging or drug agents and then reintroduced into preclinical subjects. Furthermore, since these nanoplatforms are endogenous macromolecules, they are nontoxic and completely biocompatible and biodegradable. Several studies have demonstrated the value and versatility of the lipoprotein based nanoparticles for various applications in medicine.[23-26] The goal of the present study is to investigate the utility of low-density lipoprotein (LDL) nanoparticles to access the rat brain following FUS localized opening of the BBB using the stereotaxic brain atlas method described by Bing *et al*.[27]

LDL reconstituted with the bioactive omega-3 fatty acid docosahexaenoic acid (DHA) will be examined as a novel nanomedicine for the brain.

Methods

Low-density lipoprotein

Human LDL was isolated from apheresis plasma of patients with familial hypercholesterolemia using sequential density gradient ultracentrifugation as described previously by Lund-Katz *et al.*[28].

Preparation of LDL-DHA nanoparticles

The core replacement method was used to incorporate DHA into the LDL particle.[29] Briefly, LDL freeze dried in the presence of starch was subject to several rounds of organic extraction to remove nonpolar lipids from LDL. Thereafter, DHA (dissolved in heptane) was added to the LDL residue and incubated at 4°C for 90 min. Heptane was then removed by nitrogen gas and the sample was re-suspended in 10 mM tricine buffer. Finally the sample was clarified by low-speed centrifugation, and stored under N_2 atmosphere at 4°C.

Preparation of LDL-DiR nanoparticles

Fluorescent labelled LDL was prepared by incubating the lipophilic carbocyanine dye DiR (1,1′-Dioctadecyl-3,3,3′,3′-Tetramethylindotricarbocyanine Iodide) with LDL at a molar ratio of 82:1. The reaction was carried out at 37°C for 18 h, followed by removal of excess label using ultracentrifugation (49,000 rpm for 20 h at 4°C). [30] These reaction conditions typically result in a DiR fluorophore-to–protein ratio of ∼5:1 and a protein recovery higher than 60%.

Characterization of Nanoparticles

Composition

The composition of the LDL nanoparticles was assayed for phospholipids (ferrothiocyanate reagent method)[31], free fatty acids (reverse phase-HPLC)[32] and protein (Bradford protein assay kit-Sigma). Molar concentrations of each component per particle were determined based on the assumption that one copy of the apoB-100 protein is present per LDL particle.

Mean particle size and zeta potential

The size distribution of LDL nanoparticles were evaluated by dynamic light scattering (DLS) measurements at 25°C, and the zeta potential was measured in Tricine buffer at pH 8.4 using a Zetasizer Nano (ZEN3500, Malvern Instruments, UK). All measurements were performed in at least triplicate readings**.**

Electron Microscopy Studies

Electron Microscopy was performed on a FEI Tecnai G2 Spirit transmission electron microscope equipped with a Gatan camera operating at 120 kv with Digital Micrograph software to determine the morphology and the size of the aqueous dispersion of

nanoparticles. Five microliters of lipoprotein nanoparticle suspension (~0.05 mg/ml, protein, diluted by Milli-Q water) was placed on glow-discharged carbon-coated 200 mesh copper grids and allowed to stand for 1 min. Excess sample was removed with filter paper, and repeated cycles of washing with deionized water and staining with 1% saturated aqueous uranyl acetate was performed on the grid as descried by Zhang *et al*.[33] The final stain was then drained off with filter paper, and the grid was air dried before digital images were taken.

Focused ultrasound system and stereotaxic apparatus

The system used to achieve localized BBB opening in these studies is shown in Figure 1, and was described in detail previously by Bing et al (2014). Briefly, a focused ultrasound transducer (25-mm diameter and a 20-mm radius of curvature) operating at a frequency of 1.06 MHz was used to generate pulsed acoustic exposures (burst length=10 ms, burst period=1 s, duration=120 s) in a target region of the brain upon the IV injection of microbubble contrast agents (microbubble counts 5.0-8.0×10^8/ml, Optison, GE Healthcare, Milwaukee, WI, USA). The target pressure in the brain was approximately 0.54 MPa and was determined based on a calibration of the ultrasound transducer and prior measurements of the insertion loss of the rat skull.[34] The ultrasound focus dimensions were measured to be 1.6×2×10 ± 0.1 mm (x×y×z) using a 0.2 mm needle hydrophone (HGL-0200, Onda Corporation, Sunnyvale, CA, USA). A motorized stereotaxic apparatus (51730 M, Stoelting Co., Wood Dale, IL, USA) registered to a digital rat brain atlas (StereoDrive, Neurostar, Tubingen, Germany) was used to register the x, y, z coordinates for skull sutures, bregma and lambda. Tilt correction was performed using the Neurostar software to accommodate for differences in brain size and animal position. The transducer was attached to the stereotaxic system which enable targeting of ultrasound to a specified brain region based on the atlas coordinates.

Animal Experiments

All procedures were approved by the Institutional Animal Care and Use Committee at UT Southwestern Medical Center. Female (200–270g) Sprague Dawley rats (n = 12) were used in this study. Animals were anesthetized with 2-3% isoflurane and 1-2 L/min oxygen. The lateral tail vein was catheterized using a 24-gauge catheter, and a pulse oximeter was used to monitor heart rate and oxygen saturation. A rectal temperature probe attached to a homeothermic blanket was used to record and maintain core body temperature (PhysioSuite, Kent Scientific Corp., Torrington, CT, USA). The cranial surface of the rat's skull was shaved, and a depilatory cream (VEET sensitive formula, Reckitt Benckiser, Parsippany, NJ, USA) was applied to remove fur from the surrounding area. The animal was then transferred to the stereotaxic apparatus equipped with a custom-built nose cone to deliver inhalant anesthetic. A skin incision was made over the skull to identify cranial landmarks bregma and lambda. Ultrasound gel was applied to the skull, and a custom-built water reservoir filled with degassed water was lowered over the skull for ultrasound coupling. The ultrasound probe was mounted to the stereotaxic system and a brain target (4mm to the right, 6 mm to the back and 4 mm below bregma) was selected from the digital brain atlas. The ultrasound transducer was then automatically translated such that the focus was located in this region of the brain and the pulsed exposure was delivered. First, Evans blue dye (2%; 3 ml/kg) was

injected via the tail vein catheter and allowed to circulate for a minimum of 1–3 minutes, followed by a bolus injection of microbubbles (30 μl/kg, Optison, GE Healthcare, Milwaukee, WI, USA) and nanoparticles (LDL-DHA; 100 μM or LDL-DiR; 5 μM). A 2 minute pulsed ultrasound exposure was started simultaneous with injection which lasted 120 seconds. A second identical ultrasound exposure with only microbubble administration was performed 5 minutes after the first, giving time for the first microbubble injection to clear. All brain targets were selected in the right hemisphere, while the left hemisphere was kept as a control.

For acute studies, animals were maintained under general anesthesia for 2-3 hours after the ultrasound exposure and then sacrificed, to allow for accumulation of the injected substances while the BBB was presumably open. For survival studies, animals were administered slow-release buprenorphine (0.6mg/kg SQ), recovered, and sacrificed 72 hours later. In all animals, the brains were harvested by decapitation and dissection. Brain samples that were submitted for fluorescence imaging (n=2) were placed in PBS or 10% formalin. Tissue samples that were submitted for histology (n=2) were placed in 10% buffered formalin for 24-48 hours and then sliced using a rat brain matrix (World Precision Instrument, Sarasota, FL, USA). For all samples, BBB opening was verified via the presence of Evans blue dye leakage at the target region.

Optical Fluorescence Imaging: Xenogen IVIS System

Fluorescence imaging was performed using Xenogen IVIS optical imaging system. All the tissue samples administered LDL-DiR were imaged for the detection of DiR fluorescence using excitation and emission wavelengths of 710 nm and 780 nm respectively.

Biodistribution Study: DiR Fluorescence Measurement

A biodistribution study was performed to evaluate the concentration of LDL-DiR within the body with and without the focused ultrasound exposures. Accurately weighed tissue sections were collected in glass tubes containing 1 ml phosphate buffer saline (PBS, pH 7.4). Tissues were homogenized for 30 seconds using a high speed homogenizer (PowerGen 500S1, Fisher Scientific, PA, USA) to produce a homogenous slurry. To this slurry, 2 ml of chloroform:methanol mixture (2:1) was added and vortexed thoroughly for 20 seconds. All the samples were then centrifuged at 2000 rpm for 10 min, and the chloroform layer containing DiR was collected, dried under a stream of nitrogen and re-dissolved in 1 ml chloroform. The DiR fluorescence was measured using fluorescence spectrometry (Hitachi F-7000 Fluorescence Spectrophotometer, Hitachi, CA, USA) at excitation and emission wavelengths of 710 nm and 780 nm respectively. The concentration of DiR was determined using a standard curve of DiR obtained using the same method.

Fluorescent Microscopy

Brain cryosections prepared from control animals and animals exposed to FUS/ LDL-DiR nanoparticles were mounted in ProLong Gold mounting medium containing DAPI nuclear counterstain (Invitrogen). The slides were scanned using a Zeiss Axioscan.Z1 microscope at 20× magnification using excitation and emission filter sets appropriate to detect DAPI and near-infrared signals. Exposure times were held constant for control and experimental slides

(20ms for DAPI and 1sec for DiR). Digital images were collected of the entire tissue sections and processed including adjustment of brightness and contrast of the complete images using Zeiss Zen Lite software.

DHA Quantification: Liquid Chromatography/Mass Spectrometry (LC-MS)

LC-MS was used to quantify the amount of DHA present in the brain after focused ultrasound exposures. Quantification of DHA was performed using the method reported by Aslan *et al.* [35] with slight modifications. Briefly, homogenized tissue samples were mixed with an equivalent volume of acidified acetonitrile (37% HCl) and incubated at 90°C for 2 hours to hydrolyze all esterified lipids. After this period samples were cooled to room temperature and the fatty acids were extracted with 2 ml of hexane. The organic phase was collected, dried under N2 and the residue re-suspended in a mixture of acetonitrile–water (180:20, v/v) for liquid chromatography– mass spectrometry (LC-MS) analysis. Chromatographic analysis was performed on a Waters 2998 Alliance E 2695 system with a Kinetix XB-C18 column using a step-linear gradient mobile phase composed of acetonitrile:water. DHA was identified by its specific chromatograph retention time and mass (measured on an integrated Waters Xevo QT of MS system). Finally, quantification was performed using a standard calibration curve of DHA standards.

Estimating the content of DHA in the phospholipid and free fatty acid pool within the rat brain after LDL-DHA and FUS exposure

Additional chromatography and mass spectrometry experiments were performed to determine the amount of DHA incorporated into the brain's lipids. Following IV LDL-DHA administration and FUS exposures, tissue samples from within the targeted brain regions were homogenized in PBS at a concentration of 1mg/10 μl. Brain phospholipids and unesterified fatty acids were extracted from the tissue homogenate using a simple methanol solvent system described by Zhao et al. [36] Briefly, 50 μl of tissue homogenate (derived from ∼5.0 mg of tissue) was added to 1 ml of methanol, vigorously vortexed for 1 min and incubated on ice for 10 min. Next, the mixture was centrifuged (10,000 g, 5 min, room temperature) and two portions of the supernatant (120 μl each) were dried under N2, and resuspended in an equal volume of acetonitrile. The first portion of the sample was injected into the LC/MS system described earlier to measure free DHA and intact phospholipids. The second portion of sample was subjected to acid hydrolysis with acetronitrile and HCl (as described in the previous section) for the measurement of total fatty acid content (free fatty acid and fatty acids hydrolyzed from phospholipids) by LC-MS. The difference in the LC-MS measured DHA content from the second and first samples provides an estimate of the amount of DHA incorporated in the tissue phospholipid pool.

DHA Metabolism

The following two assays were performed to monitor the metabolism of DHA to the bioactive lipid mediators, resolvin D1 and TBARS.

Resolvin Assay

Measurements of resolvin D1 (RvD1) in rat brain tissue were performed using an ELISA kit (My BioSource, San Diego, CA, USA) according to manufacturer's instructions. Briefly, tissue protein extraction reagent was added to pre-weighed tissue samples (7.5 ml per g of tissue) and homogenized for 20 seconds. Following centrifugation at 10,000 rpm for 10 min at 4°C, 100 μl of sample supernatant and rat RvD1 standards were added to each well in the ELISA plate. The plate was sealed with adhesive tape and incubated at 37°C for 90 min. Biotinylated Rat RvD1 antibody liquid was then added to each well (100 μl) and incubated for an additional 60 min at 37°C. Next, enzyme-conjugate reagent was added to each well (100 μl) and also incubated for an additional 60 min at 37°C. Finally, 100 μl of preformed color reagent A+B was added to each well incubated in the dark at 37°C. After each incubation step, the samples were washed 3 times with wash buffer. When the color for the highest concentration of the RvD1 standard curve became dark and a color gradient was visible, the reaction was stopped by adding 100 μl of preformed Color Reagent C to individual wells. The optical density was then measured at 450 nm within 10 min using a ThermoMax Microplate Reader (Molecular Devices, CA, USA) and the resolvin concentration was determined from the standard curve.

TBARS Assay

The total amount of lipid peroxidation products formed in the tissues was determined using the thiobarbituric acid (TBARS) method. [37] Briefly, brain tissue homogenates (50 μg total protein) were mixed with 1 μM copper sulfate in 5 mM HEPES (total volume 400 μl). Samples then received 1 ml of a 0.375% TBA/15% trichloroacetic acid in 0.25N HCl, incubated for 30 min at 90 °C, and were clarified by centrifugation (1500 rpm for 10 min). The resulting supernatants were aspirated and UV absorbance readings were performed at 550 nm with reference to a reagent blank. The concentration of TBARS was determined from the standard curve of malondialdehyde (MDA) and normalized to protein concentrations.

Histological Evaluation

The brains of sacrificed animals were sliced using a coronal brain-matrix slicer and were paraffin processed, embedded, and sectioned according to standard procedures within the tissue-pathology core at UT Southwestern Medical Center. Serial paraffin sections were prepared at the epicenter of FUS mediated BBB opening and stained by hematoxylin and eosin (H&E) and terminal deoxynucleotidyltransferase-mediated UTP end labeling (TUNEL). H&E-stained sections from the acute treated animals were analyzed for brain injury hallmarks such as; hemorrhage, edema, nuclear condensation, inflammatory cell infiltrate, and rarefaction. Meanwhile, TUNEL staining was performed in 72 hour survival animals to determine the presence of any possible ultrasound damage to neuronal and glial cell populations in the FUS target area. Sections subjected to TUNEL were counterstained with propidium iodide.

Results

Physicochemical Characterization: LDL-DHA and LDL-DiR

The reconstitution method used for the preparation of LDL-DHA nanoparticles produced particles with a desired particle size and uniform DHA loading (Figure 2). Dynamic light scattering analyses indicated that LDL-DHA retained a narrow particle size distribution with average particle size of 22.4 ± 0.71 nm, similar to that cited for plasma LDL. TEM also showed that these nanoparticles retained similar morphology and size as plasma LDL. The LDL-DHA nanoparticles also registered strong electronegative zeta potential readings (-25.5 ± 1.31 mV). Although these measurements are significantly different from those reported for plasma LDL (∼-8.3 mV), these values are consistent with those previously reported for LDL-DHA nanoparticles. The strong electronegative zeta potential of LDL-DHA may arise from anionic species of unesterified DHA, potentially situated in the interfacial layer of LDL.[38] Studies are ongoing in our laboratory to elucidate this finding. In terms of composition, each LDL-DHA nanoparticle contained on average 596 phospholipid molecules, 1248 molecules of DHA and a single copy of apoB-100. LDL-DHA nanoparticles do not contain any free or esterified cholesterol, as all non-polar lipids were removed during the reconstitution procedure.[39]

LDL-DiR, prepared by the co-incubation method, also retained much of the physicochemical characteristics of plasma LDL (Figure 2). LDL-DiR maintained a particle size of 20.13 ± 0.64 nm and similar morphology as plasma LDL. The zeta potential for these particles was slightly electronegative (-14.2 ± 1.4 mV, this slight change in surface charge relative to plasma LDL is typical for most modified/functionalized LDL nanoparticles.[29] The compositional make up of LDL-DiR nanoparticles contained an estimated 818 molecules of phospholipid, and 6 molecules of DiR per particle. Unlike, LDL-DHA, LDL-DiR does retain free or esterified cholesterol at its surface and in its core respectively. Although the concentrations of these sterols were not determined they are presumed to be similar to literature values for LDL.[40]

Validation of Focused ultrasound BBB Opening

The opening of BBB following FUS was confirmed by observing Evans blue staining in the targeted region of the brain. Evans blue is an azo dye that is traditionally used to assess the permeability of the BBB to macromolecules. Once injected into the blood virtually all of Evans blue dye binds to circulating serum albumin which is unable to cross the BBB. Thus, without FUS exposure the Evan's blue–albumin complex was unable to enter the brain. Administration of fluorescent LDL nanoparticles followed a similar trend (Figure 3A). Without FUS exposures only trace levels of DiR fluorescence were found in the brain after IV injection of LDL-DiR nanoparticles. The vast majority of the injected dose of LDL-DiR was taken up by the liver, spleen and adrenal glands; organs known to sequester LDL nanoparticles (Supplementary Figure 1). Conversely, when LDL-DiR was administered IV in conjunction with cerebral FUS exposure significant DiR fluorescence localized to the targeted cortical region of the brain was observed. Moreover, the fluorescence signal in the brain co-registered with the Evans blue staining. Additional microscopy studies went on to show that with FUS the LDL-DiR nanoparticles not only entered the brain, but they were

also taken up into the brain cells (Figure 3, Supplementary Figure 2). Across the FUS exposed region diffuse and punctate fluorescent staining could be seen within the cytosol of the brain cells indicating receptor mediated internalization of the LDL nanoparticles. Intense fluorescence staining was particularly evident throughout the cell body and axonal projections of neurons nearby blood vessels in the FUS exposed region. Choi *et al* reported similar findings for the spatial distribution of fluorescent dextrans after FUS mediate BBB opening.[41]

Quantitative analysis of the DiR signal in the brain regions of exposed rats revealed that the DiR fluorescence intensity in the FUS targeted region was 5-6 fold greater than that in the non-targeted contralateral hemisphere, and over 60 fold greater compared to animals receiving LDL-DiR nanoparticles without FUS exposure (Figure 3C). Collectively, these findings clearly demonstrated that FUS induced opening of the BBB can mediate LDL nanoparticle entry into the brain.

LDL-DHA Nanoparticle Delivery to the Brain

Next we sought to investigate the capability of LDL nanoparticles along with FUS exposures to deliver DHA to the rat brain. In these studies rats received either IV saline and FUS, IV LDL-DHA alone or IV LDL-DHA and FUS (Figure 4A). The IV saline and FUS controls had similar cerebral concentrations of DHA in the targeted and non-targeted hemispheres (∼3.7 ± 1.0 μmol/g) which was also similar to the concentration of DHA in the naive rat brain (3.7 ± 1.0 μmol/g). IV administration of LDL-DHA alone was unable to deliver DHA into the brain as the concentrations of DHA in both hemispheres of the brain were similar to the saline FUS controls. Unlike the previous two groups, the IV LDL-DHA and FUS exposure was able to deliver and significantly increase DHA concentration in the targeted region of the brain. The cerebral DHA levels reached 7.3 ± 2.0 μmol/g in the FUS targeted cortical regions; conversely the DHA concentrations in the non-targeted contralateral hemisphere of these rats remained similar to the control treated rats. Overall, IV LDL-DHA and FUS exposure was able to increase the levels of DHA 2-fold in the targeted region of the brain compared to non-targeted brain or control treated animals.

Further investigations into the fate of the exogenous DHA delivered to the brain via LDL nanoparticles were performed. The methanol phospholipid extractions along with LC-MS analyses revealed that the deposited unesterified DHA was readily incorporated into phospholipid membranes of the rat brain. Our calculations estimate that nearly 80% of the DHA in these brain samples was esterified in membrane phospholipids (Supplementary Figure 3). MALDI mass spectrometry of these samples confirmed these findings as we were able to detect the correct mass for phosphatidylcholine 16:0/22:6 and 18:0/22:6 at 806.5 m/z and 834.6 m/z respectively. Next, we followed the metabolism of DHA via docosanoid and TBAR analyses (Figure 4 B, C). Resolvin D1, a DHA-derived lipid mediator produced from the sequential oxygenation of DHA, was measured in each tissue sample. The levels of resolvin D1 mirrored that of DHA across the treatment groups. The control groups (IV saline/FUS and IV LDL-DHA) and the non-targeted contralateral hemisphere of the IV LDL-DHA /FUS animals all had similar levels of resolvin D1 (∼ 5.0 pg/mg tissue). The

levels of resolvin D1in the FUS targeted region of the IV LDL-DHA treated rats increased significantly to approximately 3 times that of the controls to 15.59 ± 3.3 pg/mg of tissue.

We also measured TBARS concentrations in the brain which reflect the disintegrative peroxidation of DHA and other lipids. Interestingly, cerebral TBARS levels were relatively constant across all of the treatment groups. These results demonstrate that exogenous delivery of DHA to the brain via IV LDL-DHA and FUS exposure did not induce enhanced peroxidation of DHA or increased TBARS in the FUS targeted regions of the brain.

Histological Evaluation

Finally, to assess the safety of LDL-DHA treatments and FUS exposure to the rat brain, histopathologic analysis of brains collected 3 hours and 3 days post-FUS exposure were performed. For the acute samples (3 hours post treatment), H&E analysis showed that the targeted and non-targeted regions of the brain were unremarkable (Figure 5A. There was no evidence of injury or hemorrhage in either regions of the brain. To assess more long term effects of LDL-DHA treatment and FUS exposure, TUNEL staining was performed on the samples collected 3 days after treatment/exposure. Similarly, no evidence of enhanced apoptosis or damage to DNA was seen from LDL-DHA/ FUS exposure (Figure 5B).

Discussion

Over the last two decades there has been increased interest in utilizing lipoproteins or lipoprotein-based nanoparticles as delivery platforms for diagnostic or therapeutic agents.[23-26] The vast majority of these investigational efforts have focused on non-CNS related diseases. The paucity of CNS related applications in this field arises from the difficulties of traversing these nanoparticles across the BBB for CNS delivery. The BBB effectively restricts entry of various small molecules and larger colloidal particles into the CNS. Unlike the endothelium in peripheral tissues of the body, adjacent endothelial cells in the BBB are tightly adherent, so little or no paracellular molecular diffusion occurs.[3, 4] Furthermore, these cells have essentially no fenestrae, thus little bulk phase vesicular transport take place across the BBB.[3, 4] The BBB is even restrictive to endogenous lipoproteins. Despite the need for high concentrations of cholesterol in the brain and the expression of LDL receptor (LDLR), scavenger receptor class BI (SR-BI) and ATP-binding cassette, sub-family A (ABCA1) transporters in BBB endothelial cells[42, 43], the net movement of lipoproteins from the plasma into the brain has been shown to be negligible.[44, 45] Several studies now clearly show that CNS cholesterol and lipoproteins are synthesized *de novo* within the brain.[46] Although some groups claim that lipoprotein transcytosis across BBB endothelial cells can occur[43], the contribution of this process to CNS cholesterol regulation is minor. In the present study, the BBB proved to completely restrict the entry of Evans blue dye into the brain. Similarly, the vast majority of the IV administered LDL-DiR nanoparticles were also unable to enter the brain. Only trace levels of the fluorescent LDL nanoparticle was detected in the brain, this has also been reported of other labeled LDL nanoparticles.[47] The residual amounts of LDL-DiR nanoparticles seen in the brain are likely the result of LDLR mediated transcytosis across the endothelium of the BBB. Indeed, other groups have described the active transcytosis of nanoparticles into the brain via the lipoproteins receptors present on

BBB endothelial cells.[48-50] In each of these examples circulating nanoparticles absorb exchangeable apoproteins (eg. apo-E or apo-A1) to their surface to facilitate their binding to the BBB lipoprotein receptors and entry into the brain. Despite these findings, our studies indicate this to be an inefficient transport mechanism for LDL nanoparticle delivery into the brain (Figure 3C). Most of the injected LDL nanoparticles were sequestered, as expected, by the liver, spleen and adrenal glands. To overcome the restrictions of the BBB, FUS was utilized to induce localized opening of the BBB. Following prescribed FUS exposures to the rat brain, Evans blue dye and the LDL-DiR nanoparticles were able to accumulate in the rat brain parenchyma. The intense DiR fluorescence detected in the targeted right hemisphere indicated that a considerable amount of LDL nanoparticles had entered the brain, indeed fluorometry indicated that the fluorescence intensity of the LDL-DiR nanoparticles in the targeted brain was >60 × than that of animals treated with IV LDL-DiR alone. Fluorescence microscopy experiments later showed that this fluorescence signal was detected from brain cells in the FUS exposed regions that had internalized the LDL-DiR nanoparticles. Although DiR fluorescence was greatest among cells surrounding cortical blood vessels, diffuse fluorescence staining could be seen in most the cells throughout the FUS exposed brain region, this is consistent with the fact that both glial cells and neurons express LDL receptor. [51, 52] It should be noted that small amounts of DiR fluorescence was also detected in the left contralateral hemisphere. This likely arises from the various vascular routes of interhemispheric communication in the brain (eg. anterior and posterior communicating arteries).

Our lab recently reconstituted unesterified DHA into LDL, as a new nanomedicine for cancer treatment.[29] The LDL platform proved to be an ideal carrier for DHA as it readily incorporates and solubilizes this long chain PUFA, composition analyses indicated that each LDL nanoparticle is able to carry approximately 1500 molecules of DHA.[29] Our studies went on to show that LDL-DHA nanoparticles are selectively cytotoxic to malignant murine liver cells, while non-malignant murine liver cells treated at an equivalent dose remained unharmed. [29] In addition to its anticancer properties, DHA is regarded in non-malignant cells as a nutrient that is beneficial and supportive to overall health and wellbeing. In particular, cerebral accretion of DHA is important for brain function, development and regulation of inflammation, while deficits of DHA in the brain are associated with numerous neurodegenerative diseases.[53] Given the essential and potential therapeutic role of DHA in the brain, enabling LDL mediated delivery of DHA to the brain may prove to be a valuable strategy.

Baseline levels of DHA within the rat brain were found to be approximately 3.7 μmol /gram of tissue, this is in keeping with that reported by others. [54] These levels remained unchanged when LDL-DHA nanoparticles were administered IV (without FUS exposure), thus the BBB was able to effectively restrict these nanoparticles from entering into the brain. The prescribed application of FUS and microbubbles, however, enabled LDL-DHA nanoparticles access to the brain resulting in a 2 fold increase in the DHA content in the targeted hemisphere of the brain. Thus, through the process of receptor mediated endocytosis, LDL-DHA is internalized into the brain cells and DHA will be subsequently released from the LDL during lysosomal degradation. At this point, the unesterified DHA is able to freely migrate from the lysosome to other compartments of the cell. The pool of

unesterified free fatty acid is typically maintained at low levels within the cell; as such DHA would be rapidly partitioned either to esterification or metabolism. Our studies showed that DHA delivered to the brain via LDL nanoparticles partitioned into both of these pathways. As expected DHA was readily esterified into the membrane phospholipids.[55] The brain avidly retains DHA, and studies by Singh reported that DHA comprises 40% of the PUFAs in the brain and accounts for 50% of the weight of the neuron's plasma membrane.[56] Evidence for the cerebral metabolism of DHA was demonstrated by the 3 fold increase of resolvin D1 in the FUS targeted hemisphere of the brain. Resolvin D1 is a member in the family of DHA derived lipid mediators called D-series resolvins. The synthesis of resolvins is mediated by lipoxygenase (LOX) enzymes, where DHA undergoes a sequential two-step oxidation catalyzed 15-LOX and 5-LOX to generate the resolvins.[57] In the brain, resolvins actively promote resolution to inflammatory processes.[58, 59] Known anti-inflammatory mechanisms for resolvins include the down-regulation of NF-κβ and the removal of neutrophils from inflammatory sites.[60] Often accompanying the formation of resolvins is the production of a second class of DHA derived mediators called protectins/neuroprotectins (PD/NPD1) (not analyzed herein). This group of mediators induces nerve regeneration, reduce leukocyte infiltration, and reduce pro-apoptotic and pro-inflammatory signaling.[61] Collectively, DHA derived resolvins and protectins provide potent anti-inflammatory and neuroprotective actions to the brain.

In addition to the LOX pathway, neuronal DHA could also be metabolized along free-radical mediated lipid peroxidation pathways. Lipid peroxidation, however, leads to the production of aldehyde end products that can elicit harmful effects on brain cells.[62] Enhanced lipid peroxidation, as detected by tissue TBARS, was not observed in the FUS targeted brain regions. TBARS levels were similar across all the study groups. These findings indicate that the degradative peroxidation of DHA to TBARS did not increase following LDL/FUS mediated delivery of DHA to the brain, rather DHA was preferentially oxidized through LOX system (Figure 6).

In keeping with the protective rather than cytotoxic effects of LDL-DHA, histological investigation into the acute (3 hour) and delayed (72 hours) effects of FUS and LDL-DHA exposure on the brain was unremarkable. No evidence of acute neuronal damage or capillary hemorrhage in the prescribed brain regions exposed to FUS and LDL-DHA nanoparticles were observed. Similarly, TUNEL stain performed on the brain sections 72 hours post FUS and LDL-DHA exposure did not show any signs of cell death or DNA damage.

In summary, we have demonstrated that stereotactic-guided FUS is able to noninvasively mediate the entry of LDL nanoparticles into the normal rat brain. The LDL nanoparticles were selectively taken up into the brain cells in the targeted region of FUS exposure. In the case of the LDL-DHA nanoparticles, once endocytosed, DHA was readily incorporated into the brain cells phospholipid membranes. In addition to esterification, the LDL delivered DHA was also preferentially oxidized to the pro-resolving lipid mediator resolvin D1, rather than undergoing lipid peroxidation to MDA. DHA supplementation to the brain is of clinical interest to many as DHA is implicated in providing numerous neurological benefits.[63] DHA accretion into the brain from dietary supplementation is relatively slow (∼4mg per day).[64] Thus, in conditions where the brain's DHA content (normal average 5 g)[64] is

deficient by 20-30% (which is typically seen with brain disorders), it would take many months to over a year to replenish the DHA levels through dietary intake. Here, we show that FUS/LDL-DHA nanoparticle exposures can double the content of DHA in prescribed regions of the brain in a matter of hours. Hence, in accordance with former studies that have examined the role of omega-3 fatty acids in the CNS, LDL mediated delivery of DHA to the brain should improve cognition[65], reduce neuroinflammation[66], and protect against seizures[67] and strokes[68]. In addition, DHA has been implicated imparting anticancer effects[69, 70]; hence this particle may also play a role in the treatment of brain tumors. One of the main uncertainties of this approach is the neurological consequence associated with repeat opening of the BBB using focused ultrasound. The chronic nature of neurodegenerative diseases would require repetitive opening of the BBB for the LDL-DHA treatment. Preliminary studies imply safety of repeat BBB opening, but further studies are necessary.[71] This technology may be better utilized in acute conditions of brain injury where a single intervention of FUS/LDL-DHA exposure could protect the brain by limiting the neuroinflammatory cascade and facilitating the resolution at the sites of injury.[66, 72] Studies are ongoing in our lab to assess the utility of FUS/LDL-DHA nanoparticle technology in these clinical settings.

Supplementary Material

Refer to Web version on PubMed Central for supplementary material.

Acknowledgments

This work was supported in part by the Cancer Prevention and Research Initiative of Texas (R1308), the Southwestern Small Animal Imaging Research Program (SW-SAIRP) (NCI U24 CA126608), and the Cancer Center Support Grant (5P30 CA 142543-05). We would also like to thank the UTSW Whole Brain Microscopy Facility (WBMF) in the Department of Neurology and Neurotherapeutics for assistance with slide scanning. WBMF is supported by the Texas Institute for Brain Injury and Repair (TIBIR). The authors would also like to acknowledge the technical assistance from Debra Szczepanski and graphic illustrations from Malvika Kumar. The authors of this study have no conflicts of interest to report.

References

1. Pardridge WM. Drug transport across the blood-brain barrier. Journal of cerebral blood flow and metabolism : official journal of the International Society of Cerebral Blood Flow and Metabolism. 2012; 32:1959–72.
2. Rubin LL, Staddon JM. The cell biology of the blood-brain barrier. Annual review of neuroscience. 1999; 22:11–28.
3. Stewart PA, Hayakawa EM. Interendothelial junctional changes underlie the developmental ‘tightening’ of the blood-brain barrier. Brain research. 1987; 429:271–81. [PubMed: 3567665]
4. Wolburg H, Lippoldt A. Tight junctions of the blood-brain barrier: development, composition and regulation. Vascular pharmacology. 2002; 38:323–37. [PubMed: 12529927]
5. Pardridge WM. Blood-brain barrier drug targeting: the future of brain drug development. Molecular interventions. 2003; 3:90–105. 51. [PubMed: 14993430]
6. Cosolo WC, Martinello P, Louis WJ, Christophidis N. Blood-brain barrier disruption using mannitol: time course and electron microscopy studies. The American journal of physiology. 1989; 256:R443–7. [PubMed: 2492773]
7. Zou L-L, Ma J-L, Wang T, Yang T-B, Liu C-B. Cell-Penetrating Peptide-Mediated Therapeutic Molecule Delivery into the Central Nervous System. Current Neuropharmacology. 2013; 11:197–208. [PubMed: 23997754]

8. Bobo RH, Laske DW, Akbasak A, Morrison PF, Dedrick RL, Oldfield EH. Convection-enhanced delivery of macromolecules in the brain. Proceedings of the National Academy of Sciences. 1994; 91:2076–80.
9. Fresta M, Puglisi G. Survival rate improvement in a rat ischemia model by long circulating liposomes containing cytidine-5I-diphosphate choline. Life sciences. 1997; 61:1227–35. [PubMed: 9324064]
10. Korkusuz H, Ulbrich K, Welzel K, Koeberle V, Watcharin W, Bahr U, et al. Transferrin-coated gadolinium nanoparticles as MRI contrast agent. Molecular imaging and biology : MIB : the official publication of the Academy of Molecular Imaging. 2013; 15:148–54. [PubMed: 22811020]
11. Kreuter J. Influence of chronobiology on the nanoparticle-mediated drug uptake into the brain. Pharmaceutics. 2015; 7:3–9. [PubMed: 25654637]
12. Cosco D, Di Marzio L, Marianecci C, Trapasso E, Paolino D, Celia C, et al. Colloidal Supramolecular Aggregates for Therapeutic Application in Neuromedicine. Current Medicinal Chemistry. 2014; 21:4132–53. [PubMed: 25174931]
13. Hynynen K, McDannold N, Vykhodtseva N, Jolesz FA. Noninvasive MR imaging-guided focal opening of the blood-brain barrier in rabbits. Radiology. 2001; 220:640–6. [PubMed: 11526261]
14. Sheikov N, McDannold N, Vykhodtseva N, Jolesz F, Hynynen K. Cellular mechanisms of the blood-brain barrier opening induced by ultrasound in presence of microbubbles. Ultrasound in medicine & biology. 2004; 30:979–89. [PubMed: 15313330]
15. Marty B, Larrat B, Van Landeghem M, Robic C, Robert P, Port M, et al. Dynamic study of blood-brain barrier closure after its disruption using ultrasound: a quantitative analysis. Journal of cerebral blood flow and metabolism : official journal of the International Society of Cerebral Blood Flow and Metabolism. 2012; 32:1948–58.
16. Cho EE, Drazic J, Ganguly M, Stefanovic B, Hynynen K. Two-photon fluorescence microscopy study of cerebrovascular dynamics in ultrasound-induced blood-brain barrier opening. Journal of cerebral blood flow and metabolism : official journal of the International Society of Cerebral Blood Flow and Metabolism. 2011; 31:1852–62.
17. Park J, Zhang Y, Vykhodtseva N, Jolesz FA, McDannold NJ. The kinetics of blood brain barrier permeability and targeted doxorubicin delivery into brain induced by focused ultrasound. J Control Release. 2012; 162:134–42. [PubMed: 22709590]
18. Hynynen K, McDannold N, Vykhodtseva N, Jolesz FA. Non-invasive opening of BBB by focused ultrasound. Acta neurochirurgica Supplement. 2003; 86:555–8. [PubMed: 14753505]
19. Chen H, Konofagou EE. The size of blood-brain barrier opening induced by focused ultrasound is dictated by the acoustic pressure. Journal of cerebral blood flow and metabolism : official journal of the International Society of Cerebral Blood Flow and Metabolism. 2014; 34:1197–204.
20. De Jong WH, Borm PJA. Drug delivery and nanoparticles: Applications and hazards. International Journal of Nanomedicine. 2008; 3:133–49. [PubMed: 18686775]
21. Palombo M, Deshmukh M, Myers D, Gao J, Szekely Z, Sinko PJ. Pharmaceutical and Toxicological Properties of Engineered Nanomaterials for Drug Delivery. Annual Review of Pharmacology and Toxicology. 2014; 54:581–98.
22. Masserini M. Nanoparticles for Brain Drug Delivery. ISRN Biochemistry. 2013; 2013:18.
23. Corbin IR, Li H, Chen J, Lund-Katz S, Zhou R, Glickson JD, et al. Low-density lipoprotein nanoparticles as magnetic resonance imaging contrast agents. Neoplasia. 2006; 8:488–98. [PubMed: 16820095]
24. Duivenvoorden R, Tang J, Cormode DP, Mieszawska AJ, Izquierdo-Garcia D, Ozcan C, et al. A statin-loaded reconstituted high-density lipoprotein nanoparticle inhibits atherosclerotic plaque inflammation. Nat Commun. 2014; 5
25. Ng KK, Lovell JF, Zheng G. Lipoprotein-inspired nanoparticles for cancer theranostics. Acc Chem Res. 2011; 44:1105–13. [PubMed: 21557543]
26. Allijn IE, Leong W, Tang J, Gianella A, Mieszawska AJ, Fay F, et al. Gold Nanocrystal Labeling Allows Low-Density Lipoprotein Imaging from the Subcellular to Macroscopic Level. ACS Nano. 2013; 7:9761–70. [PubMed: 24127782]

27. Bing C, Ladouceur-Wodzak M, Wanner CR, Shelton JM, Richardson JA, Chopra R. Trans-cranial opening of the blood-brain barrier in targeted regions using a stereotaxic brain atlas and focused ultrasound energy. Journal of therapeutic ultrasound. 2014; 2:13. [PubMed: 25232482]
28. Lund-Katz S, Laplaud PM, Phillips MC, Chapman MJ. Apolipoprotein B-100 conformation and particle surface charge in human LDL subspecies: implication for LDL receptor interaction. Biochemistry. 1998; 37:12867–74. [PubMed: 9737865]
29. Reynolds L, Mulik RS, Wen X, Dilip A, Corbin IR. Low-density lipoprotein-mediated delivery of docosahexaenoic acid selectively kills murine liver cancer cells. Nanomedicine- Uk. 2014:1–19.
30. Li H, Zhang Z, Blessington D, Nelson DS, Zhou R, Lund-Katz S, et al. Carbocyanine labeled LDL for optical imaging of tumors. Acad Radiol. 2004; 11:669–77. [PubMed: 15172369]
31. Stewart JC. Colorimetric determination of phospholipids with ammonium ferrothiocyanate. Anal Biochem. 1980; 104:10–4. [PubMed: 6892980]
32. Mehta A, Oeser AM, Carlson MG. Rapid quantitation of free fatty acids in human plasma by high-performance liquid chromatography. J Chromatogr B Biomed Sci Appl. 1998; 719:9–23. [PubMed: 9869359]
33. Zhang L, Tong H, Garewal M, Ren G. Optimized negative-staining electron microscopy for lipoprotein studies. Biochim Biophys Acta. 2013; 1830:2150–9. [PubMed: 23032862]
34. O'Reilly MA, Muller A, Hynynen K. Ultrasound Insertion Loss of Rat Parietal Bone Appears to Be Proportional to Animal Mass at. Submegahertz Frequencies Ultrasound in Medicine and Biology. 37:1930–7. [PubMed: 21925788]
35. Aslan M, Ozcan F, Aslan I, Yucel G. LC-MS/MS analysis of plasma polyunsaturated fatty acids in type 2 diabetic patients after insulin analog initiation therapy. Lipids in health and disease. 2013; 12:169. [PubMed: 24195588]
36. Zhao Z, Xu Y. An extremely simple method for extraction of lysophospholipids and phospholipids from blood samples. Journal of Lipid Research. 2010; 51:652–9. [PubMed: 19783525]
37. Erdahl WL, Krebsbach RJ, Pfeiffer DR. A comparison of phospholipid degradation by oxidation and hydrolysis during the mitochondrial permeability transition. Archives of Biochemistry and Biophysics. 1991; 285:252–60. [PubMed: 1897931]
38. Aggerbeck LP, Kezdy FJ, Scanu AM. Enzymatic probes of lipoprotein structure. Hydrolysis of human serum low density lipoprotein-2 by phospholipase A2. J Biol Chem. 1976; 251:3823–30. [PubMed: 180009]
39. Krieger M, McPhaul MJ, Goldstein JL, Brown MS. Replacement of neutral lipids of low density lipoprotein with esters of long chain unsaturated fatty acids. J Biol Chem. 1979; 254:3845–53. [PubMed: 220222]
40. Shen BW, Scanu AM, Kezdy FJ. Structure of human serum lipoproteins inferred from compositional analysis. Proc Natl Acad Sci U S A. 1977; 74:837–41. [PubMed: 265578]
41. Choi JJ, Wang S, Tung YS, Morrison B 3rd, Konofagou EE. Molecules of various pharmacologically-relevant sizes can cross the ultrasound-induced blood-brain barrier opening in vivo. Ultrasound in medicine & biology. 2010; 36:58–67. [PubMed: 19900750]
42. Panzenboeck U, Balazs Z, Sovic A, Hrzenjak A, Levak-Frank S, Wintersperger A, et al. ABCA1 and scavenger receptor class B, type I, are modulators of reverse sterol transport at an in vitro blood-brain barrier constituted of porcine brain capillary endothelial cells. J Biol Chem. 2002; 277:42781–9. [PubMed: 12202492]
43. Dehouck B, Fenart L, Dehouck MP, Pierce A, Torpier G, Cecchelli R. A new function for the LDL receptor: transcytosis of LDL across the blood-brain barrier. J Cell Biol. 1997; 138:877–89. [PubMed: 9265653]
44. Spady DK, Huettinger M, Bilheimer DW, Dietschy JM. Role of receptor-independent low density lipoprotein transport in the maintenance of tissue cholesterol balance in the normal and WHHL rabbit. J Lipid Res. 1987; 28:32–41. [PubMed: 3559399]
45. Osono Y, Woollett LA, Herz J, Dietschy JM. Role of the low density lipoprotein receptor in the flux of cholesterol through the plasma and across the tissues of the mouse. J Clin Invest. 1995; 95:1124–32. [PubMed: 7883961]

46. Dietschy JM, Turley SD. Thematic review series: brain Lipids. Cholesterol metabolism in the central nervous system during early development and in the mature animal. J Lipid Res. 2004; 45:1375–97. [PubMed: 15254070]
47. Spady DK, Bilheimer DW, Dietschy JM. Rates of receptor-dependent and -independent low density lipoprotein uptake in the hamster. Proc Natl Acad Sci U S A. 1983; 80:3499–503. [PubMed: 6304713]
48. Goppert TM, Muller RH. Polysorbate-stabilized solid lipid nanoparticles as colloidal carriers for intravenous targeting of drugs to the brain: comparison of plasma protein adsorption patterns. J Drug Target. 2005; 13:179–87. [PubMed: 16036306]
49. Kreuter J, Hekmatara T, Dreis S, Vogel T, Gelperina S, Langer K. Covalent attachment of apolipoprotein A-I and apolipoprotein B-100 to albumin nanoparticles enables drug transport into the brain. J Control Release. 2007; 118:54–8. [PubMed: 17250920]
50. Lemke A, Kiderlen AF, Petri B, Kayser O. Delivery of amphotericin B nanosuspensions to the brain and determination of activity against Balamuthia mandrillaris amebas. Nanomedicine-Uk. 2010; 6:597–603.
51. Herz J, Beffert U. Apolipoprotein E receptors: linking brain development and Alzheimer's disease. Nature reviews Neuroscience. 2000; 1:51–8. [PubMed: 11252768]
52. Jung-Testas I, Weintraub H, Dupuis D, Eychenne B, Baulieu EE, Robel P. Low density lipoprotein-receptors in primary cultures of rat glial cells. The Journal of steroid biochemistry and molecular biology. 1992; 42:597–605. [PubMed: 1637723]
53. Bazinet RP, Laye S. Polyunsaturated fatty acids and their metabolites in brain function and disease. Nature reviews Neuroscience. 2014; 15:771–85. [PubMed: 25387473]
54. Domenichiello AF, Chen CT, Trepanier MO, Stavro PM, Bazinet RP. Whole body synthesis rates of DHA from alpha-linolenic acid are greater than brain DHA accretion and uptake rates in adult rats. J Lipid Res. 2014; 55:62–74. [PubMed: 24212299]
55. Crawford MA, Bloom M, Broadhurst CL, Schmidt WF, Cunnane SC, Galli C, et al. Evidence for the unique function of docosahexaenoic acid during the evolution of the modern hominid brain. Lipids. 1999; 34(Suppl):S39–47. [PubMed: 10419087]
56. Singh M. Essential fatty acids, DHA and human brain. Indian journal of pediatrics. 2005; 72:239–42. [PubMed: 15812120]
57. Hong S, Gronert K, Devchand PR, Moussignac RL, Serhan CN. Novel docosatrienes and 17S-resolvins generated from docosahexaenoic acid in murine brain, human blood, and glial cells. Autacoids in anti-inflammation. J Biol Chem. 2003; 278:14677–87. [PubMed: 12590139]
58. Serhan CN, Brain SD, Buckley CD, Gilroy DW, Haslett C, O'Neill LA, et al. Resolution of inflammation: state of the art, definitions and terms. FASEB J. 2007; 21:325–32. [PubMed: 17267386]
59. Serhan CN. Resolution phase of inflammation: novel endogenous anti-inflammatory and proresolving lipid mediators and pathways. Annual review of immunology. 2007; 25:101–37.
60. Tassoni D, Kaur G, Weisinger RS, Sinclair AJ. The role of eicosanoids in the brain. Asia Pacific journal of clinical nutrition. 2008; 17(Suppl 1):220–8. [PubMed: 18296342]
61. Niemoller TD, Bazan NG. Docosahexaenoic acid neurolipidomics. Prostaglandins & other lipid mediators. 2010; 91:85–9. [PubMed: 19804838]
62. Esterbauer H, Schaur RJ, Zollner H. Chemistry and biochemistry of 4-hydroxynonenal, malonaldehyde and related aldehydes. Free Radical Biology and Medicine. 1991; 11:81–128. [PubMed: 1937131]
63. Dyall SC, Michael-Titus AT. Neurological benefits of omega-3 fatty acids. Neuromolecular medicine. 2008; 10:219–35. [PubMed: 18543124]
64. Rapoport SI, Rao JS, Igarashi M. Brain metabolism of nutritionally essential polyunsaturated fatty acids depends on both the diet and the liver. Prostaglandins, Leukotrienes and Essential Fatty Acids. 2007; 77:251–61.
65. Barberger-Gateau P, Letenneur L, Deschamps V, Peres K, Dartigues JF, Renaud S. Fish, meat, and risk of dementia: cohort study. Bmj. 2002; 325:932–3. [PubMed: 12399342]

66. Orr SK, Palumbo S, Bosetti F, Mount HT, Kang JX, Greenwood CE, et al. Unesterified docosahexaenoic acid is protective in neuroinflammation. Journal of neurochemistry. 2013; 127:378–93. [PubMed: 23919613]

67. Trepanier MO, Taha AY, Mantha RL, Ciobanu FA, Zeng QH, Tchkhartichvili GM, et al. Increases in seizure latencies induced by subcutaneous docosahexaenoic acid are lost at higher doses. Epilepsy research. 2012; 99:225–32. [PubMed: 22285511]

68. Bazan NG, Molina MF, Gordon WC. Docosahexaenoic acid signalolipidomics in nutrition: significance in aging, neuroinflammation, macular degeneration, Alzheimer's, and other neurodegenerative diseases. Annu Rev Nutr. 2011; 31:321–51. [PubMed: 21756134]

69. Gleissman H, Yang R, Martinod K, Lindskog M, Serhan CN, Johnsen JI, et al. Docosahexaenoic acid metabolome in neural tumors: identification of cytotoxic intermediates. FASEB J. 2010; 24:906–15. [PubMed: 19890019]

70. Lindskog M, Gleissman H, Ponthan F, Castro J, Kogner P, Johnsen JI. Neuroblastoma cell death in response to docosahexaenoic acid: sensitization to chemotherapy and arsenic-induced oxidative stress. Int J Cancer. 2006; 118:2584–93. [PubMed: 16353135]

71. Downs ME, Buch A, Sierra C, Karakatsani ME, Chen S, Konofagou EE, et al. Long-Term Safety of Repeated Blood-Brain Barrier Opening via Focused Ultrasound with Microbubbles in Non-Human Primates Performing a Cognitive Task. PLoS One. 2015; 10:e0125911. [PubMed: 25945493]

72. Belayev L, Marcheselli VL, Khoutorova L, Rodriguez de Turco EB, Busto R, Ginsberg MD, et al. Docosahexaenoic acid complexed to albumin elicits high-grade ischemic neuroprotection. Stroke; a journal of cerebral circulation. 2005; 36:118–23.

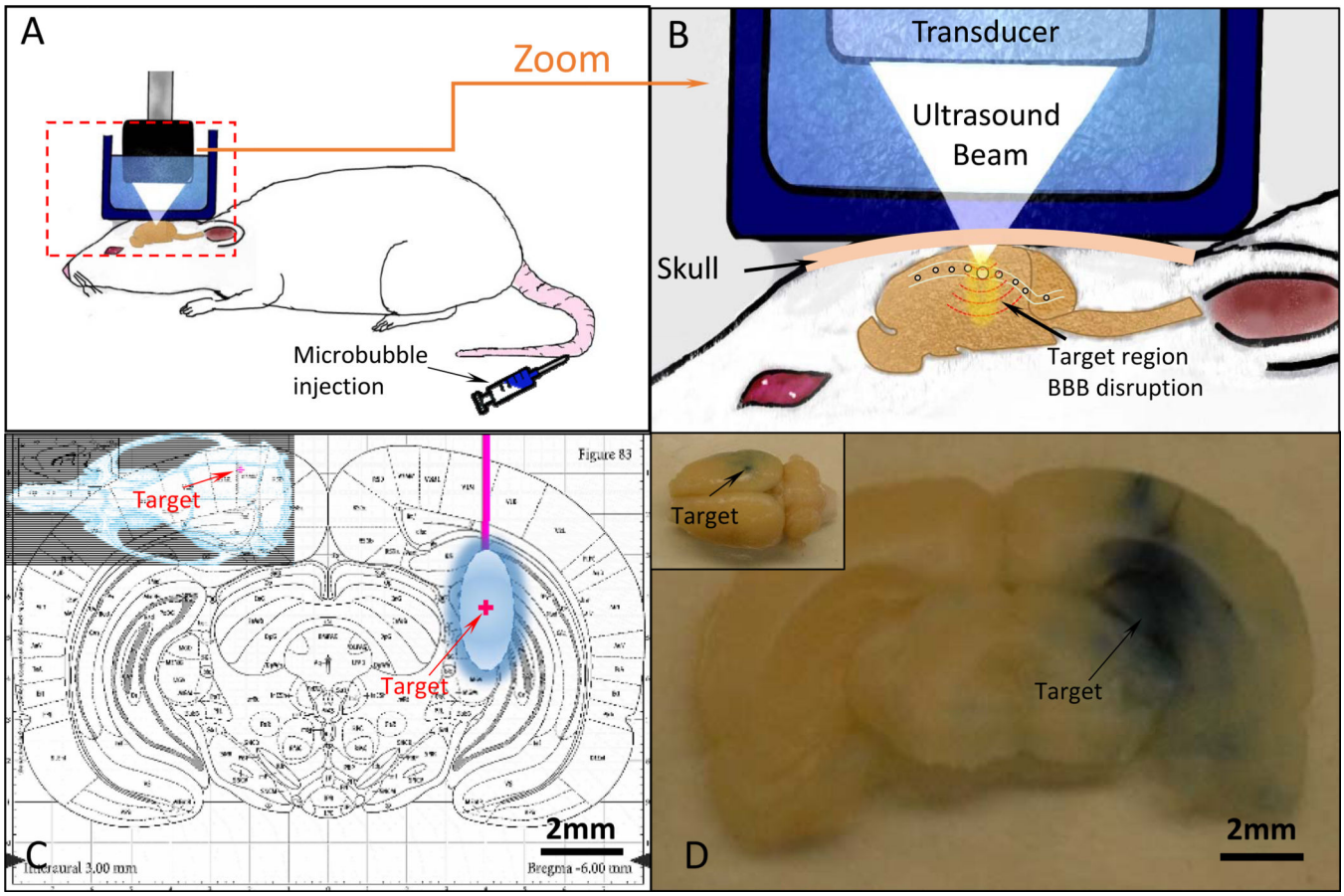

Figure 1. Stereotaxic System and FUS Set Up

A. Schematic showing the method of achieving localized BBB opening in a rat model using pulsed ultrasound exposures and intravenous microbubbles. B. A close up view of the brain depicts how microbubbles flowing through the brain vasculature respond to the pressure variation produced by the ultrasound exposures to achieve localized BBB opening. C. The target brain location for all animals in this study is overlaid on the transverse brain atlas slice. D. A corresponding brain slice harvested from an animal exposed to ultrasound shows localized leakage of Evans blue into the corresponding brain region.

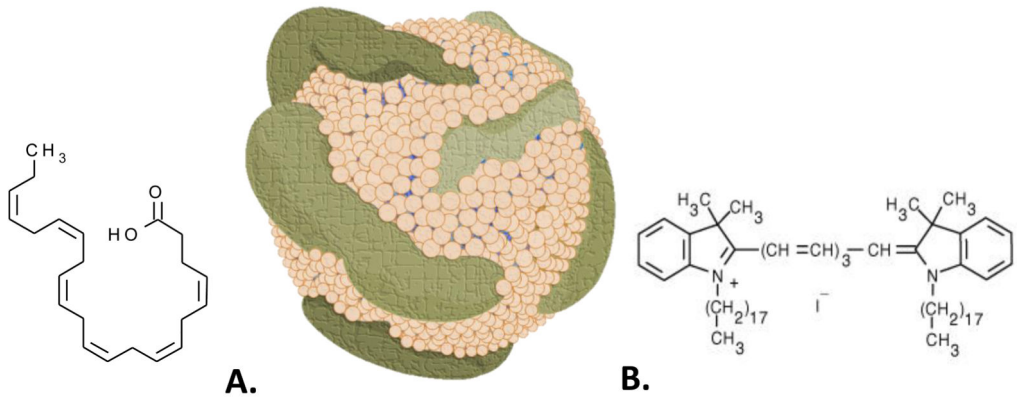

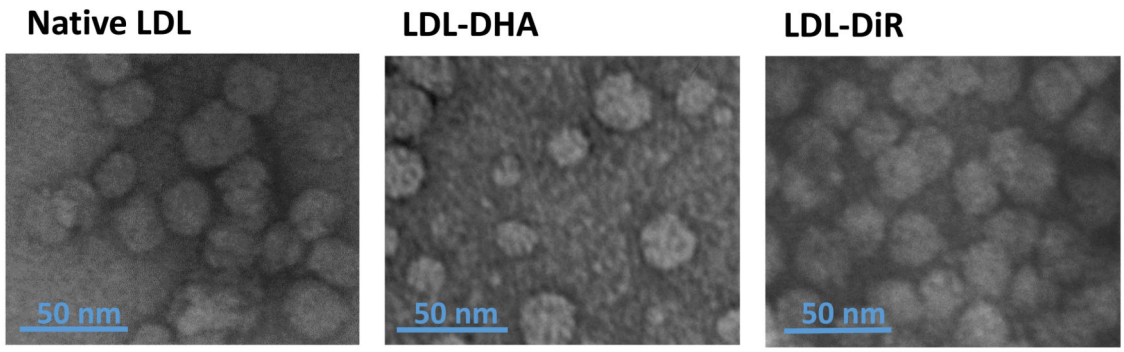

	Native LDL	LDL-DHA	LDL-DiR
ApoB-100	1	1	1
Phospholipid (moles)	673.9 ± 101.6	595.7 ± 80.0	818.2 ± 93.8
Cholesterol (moles)	2958 ± 378*	ND	ND
Lipid Cargo (moles)	**	1248.3 ± 110.4†	5.65 ± 0.7‡
Diameter (nm)	17.75 ± 0.5	22.4 ± 0.7	20.13 ± 0.6
Surface Charge (mV)	-9.1 ± 0.9	-25.5 ± 1.3	-14.24 ± 1.5

Figure 2. LDL Nanoparticle

Above, Schematic drawing of LDL nanoparticle alongside structures of DHA (A) and DIR (B). Middle, Transmission electron microscopy of native LDL and LDL nanoparticles. Below, Characterization table containing composition and physicochemical properties of native LDL and LDL nanoparticles. Total cholesterol includes cholesteryl esters and free cholesterol. Literature values indicate that LDL typically carries between 1300-1600 cholestryl esters and 500-600 free cholesterol molecules. ** LDL also carries about 170 triglyceride molecules. DHA typically makes up only 1% of the total fatty acid composition

of LDL. † DHA cargo; ‡ DiR cargo. ND, not determined. LDL-DHA do not contain any neutral lipids. LDL-DiR contains full complement of neutral lipids.

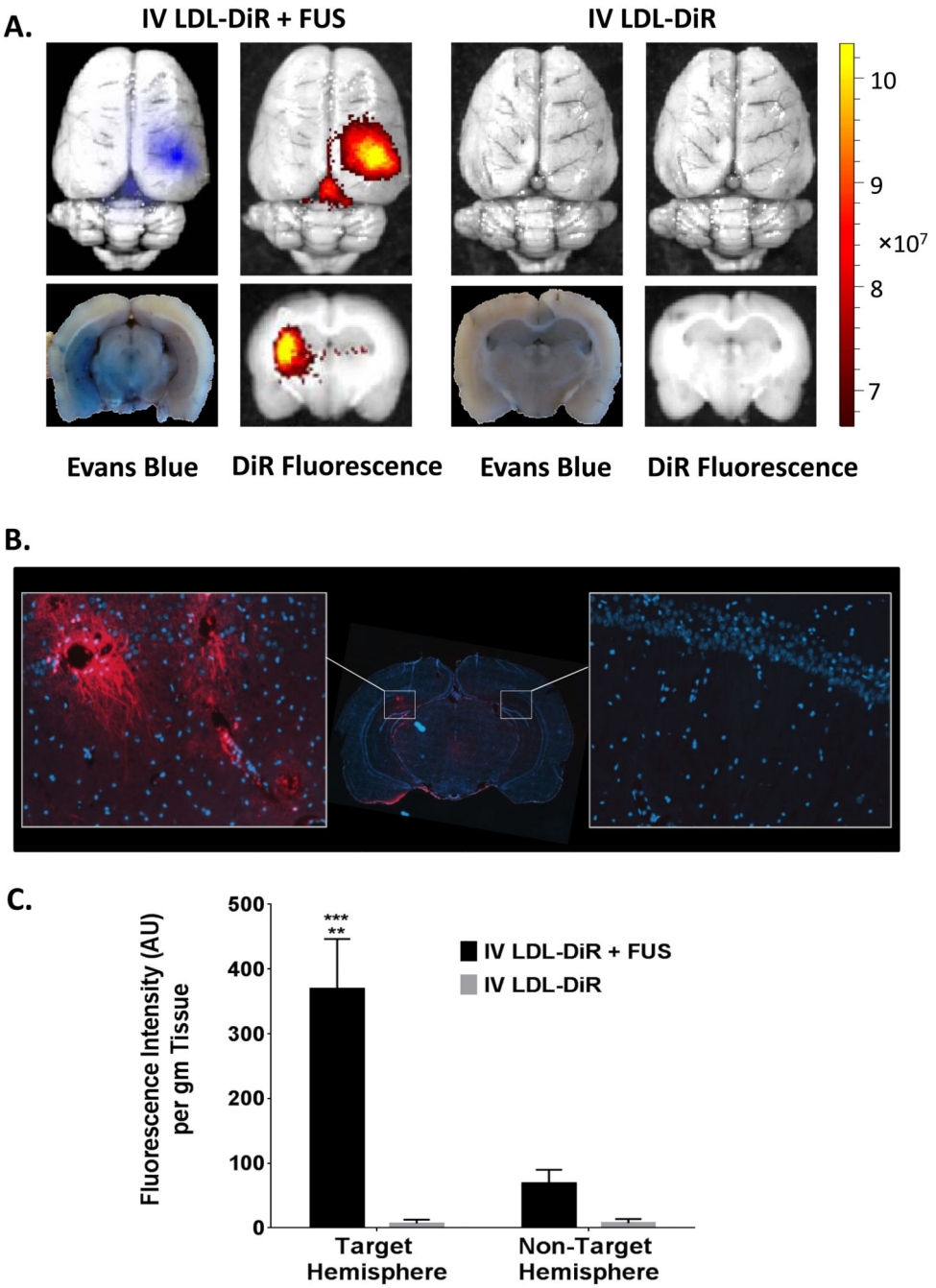

Figure 3. LDL-DiR Uptake into the Brain after FUS: Fluorescence Imaging

Xenogen IVIS optical imaging was used to track the DiR fluorescence in the brain. A. Whole brain (top) and cross-section (bottom) of brain from rats injected intravenous with LDL-DiR in presence or absence of FUS. B. **Fluorescence Microscopy**. Digital fluorescent image from coronal cryosection of the brain. Representative areas of interest are expanded from FUS exposed region (left) and contralateral hemisphere (right). Images were captured at 20× magnification. C. **Fluorescence Spectrometry.** Quantitative measurement of DiR fluorescence in the brain (AU per g of tissue) treated with IV LDL-DiR + FUS and IV LDL-

DiR was determined by fluorescence spectrometry at λex and λem of 710 nm and 780 nm respectively (n=3). (**), (***) represent a significant difference from the corresponding groups at $p<0.005$ and $p<0.001$ respectively.

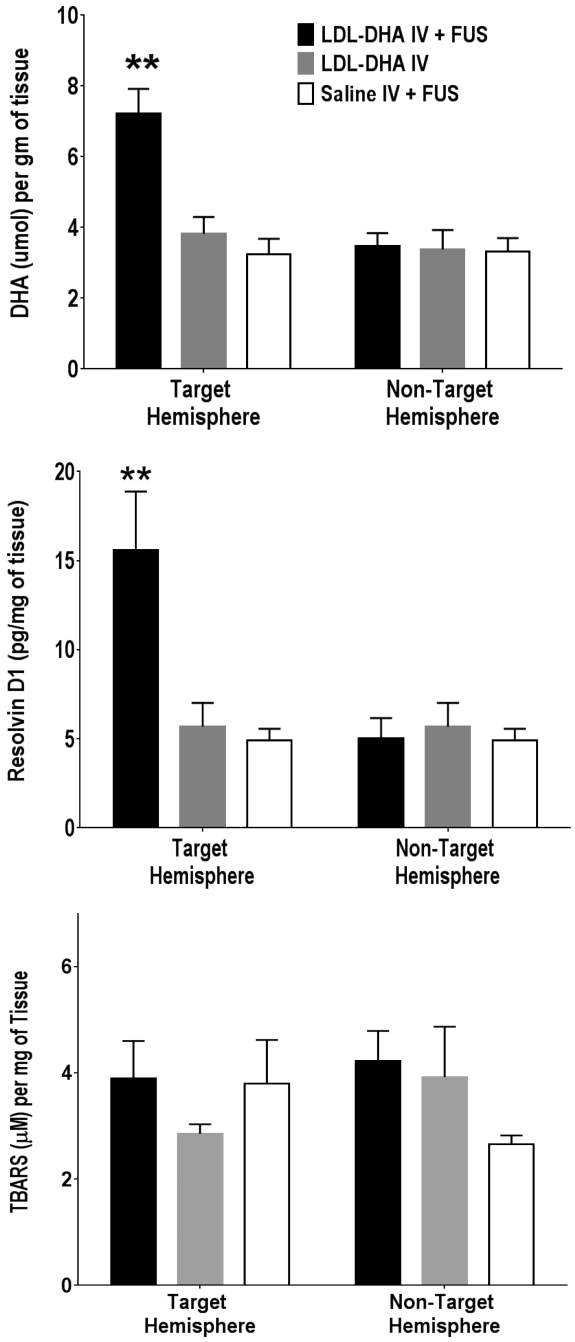

Figure 4. Quantification of DHA Metabolites. A. Measurements of DHA

The amount of DHA in different brain samples (IV LDL-DHA + FUS, IV LDL-DHA and IV Saline + FUS) was determined using LC-MS (n=3). The DHA values are presented as μmol of DHA per g of tissue. **B. Measurement of Resolvin D1.** The amount of DHA derived Resolvin D1 produced in different brain samples (IV LDL-DHA + FUS, IV LDL-DHA and IV Saline) was determined using a Rat resolvin D1 ELISA kit (n=3). The resolvin values are presented as pg of resolving D1 per mg of tissue). **C. Measurement of Lipid Peroxidation** The effect of IV LDL-DHA + FUS, IV LDL-DHA and IV Saline treatments

on lipid peroxidation levels was determined using TBARS assay (n=3). The TBARS values are presented as μM of TBARS per mg of tissue. (**) represent a significant difference from the corresponding groups at $p<0.005$.

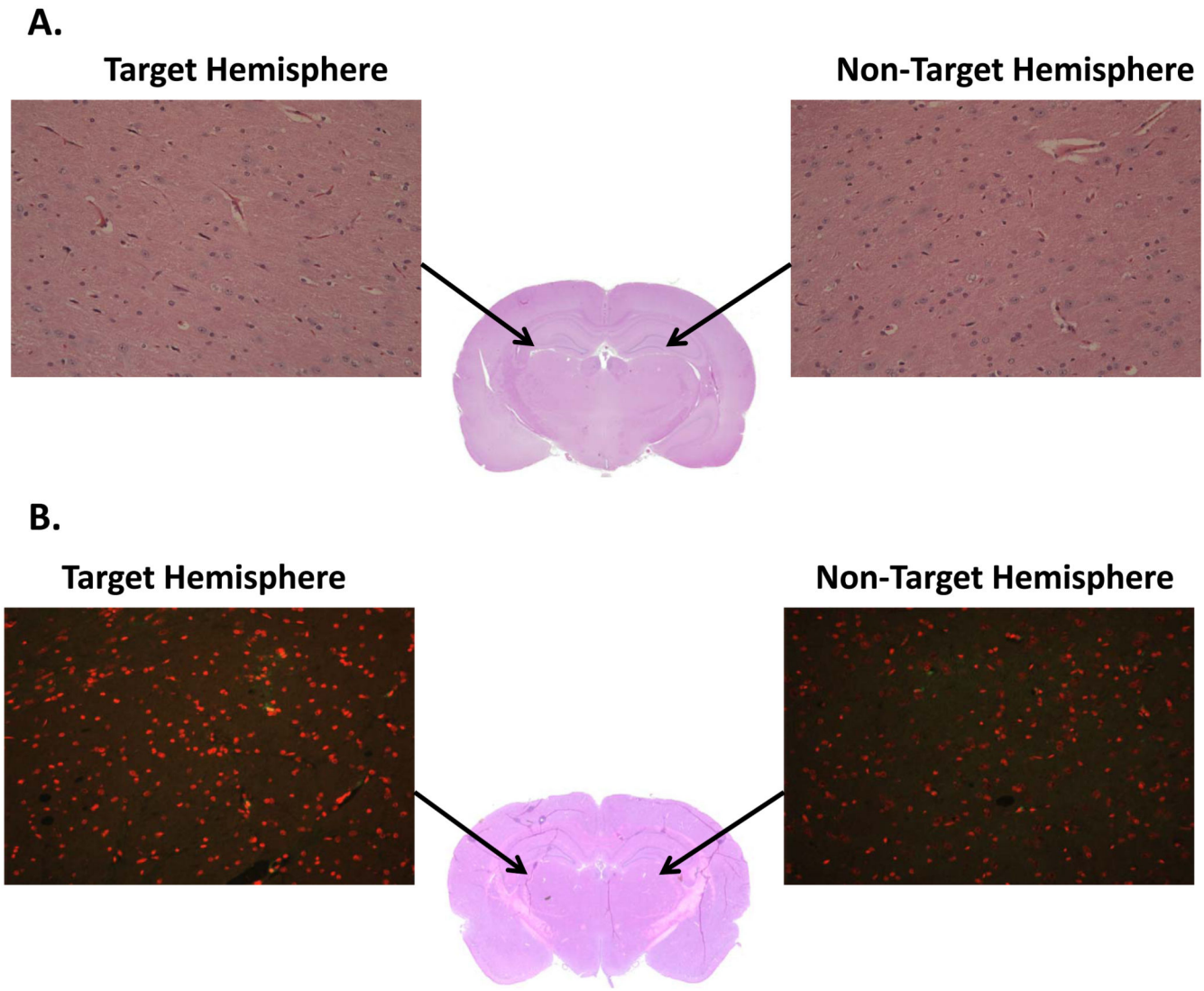

Figure 5. Histology Investigation A. Effect of FUS and Acute Treatment of LDL-DHA
This study was performed using H and E staining to determine any brain damage (such as; hemorrhage, edema, nuclear condensation) by FUS and acute treatment of LDL-DHA to the ultrasound focused area as well as whole brain. **B. TUNEL Assay: Effect of FUS and Chronic Treatment of LDL-DHA** This study was performed using TUNEL staining to determine any damage by FUS and chronic treatment of LDL-DHA to the neuronal and glial cells in the ultrasound focused area as well as whole brain of acute LDL-DHA treatment. Arrows indicate area of focus.

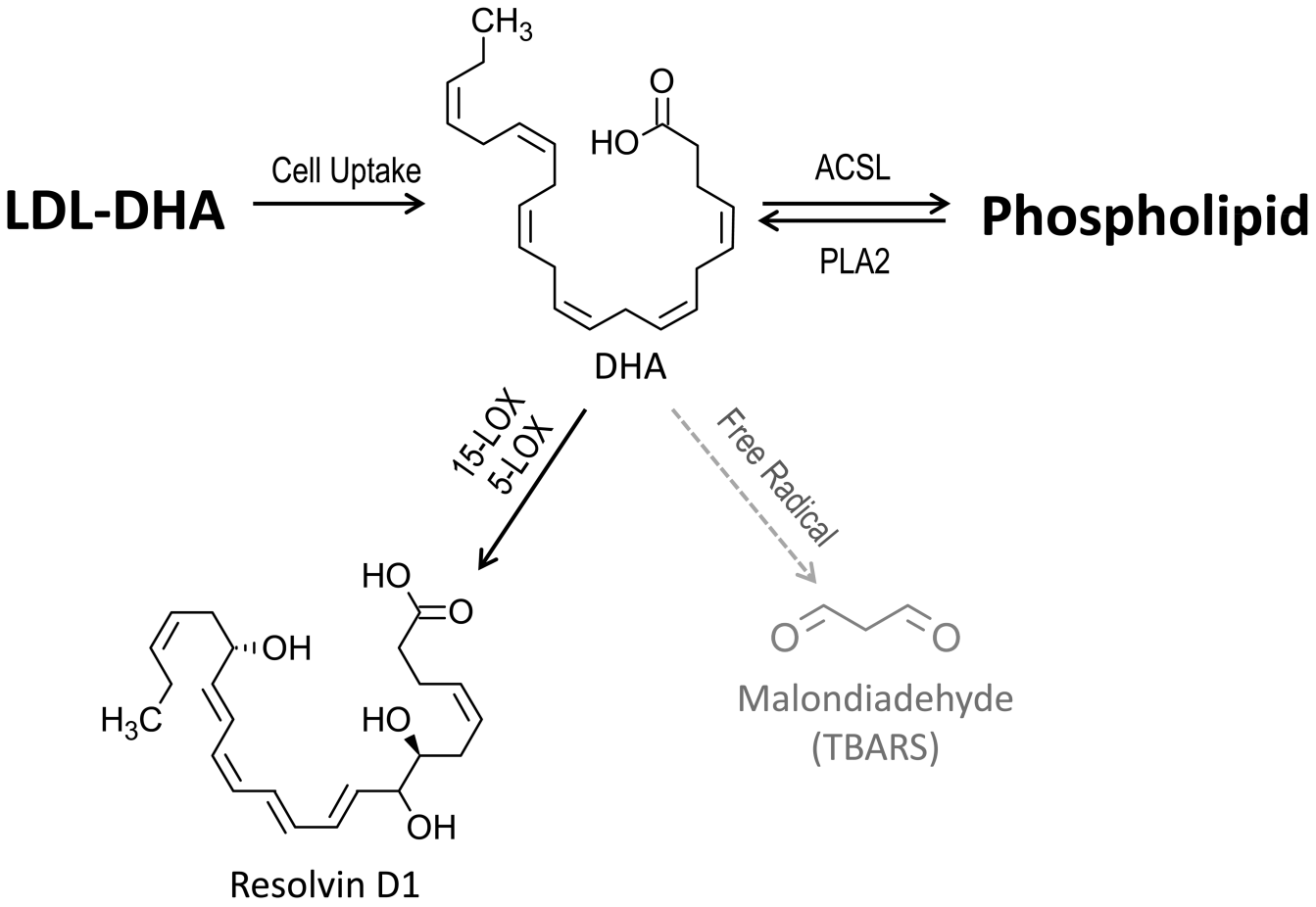

Figure 6. LDL-DHA Metabolism

Following intracellular uptake by the LDL receptor, DHA is liberated from the LDL nanoparticle. Unesterified DHA can be: activated by Long-chain-fatty-acid— CoA ligase (ACSL) for esterification into sn2 position in membrane phospholipids; metabolized sequentially via lipoxygenase enzyme system to resolvins; or alternatively, undergo free radical mediated lipid peroxidation to aldehyde end products. DHA delivered to the brain by the LDL nanoparticles preferentially undergoes oxidation via the lipoxygenase pathway rather than free radical degradation. PLA2, phospholipase A2; 15-LOX, 15-lipoxygenase; 5-LOX, 5-lipoxygenase; TBARS, thiobartuic reactive substances.